

Supporting Information

for

Electronic State Mixing Controls the Photoreactivity of a Rhodopsin with all-*trans* Chromophore Analogues

Madushanka Manathunga[†], Xuchun Yang[†] and Massimo Olivucci^{†,¶,‡}

[†]Department of Chemistry, Bowling Green State University, Bowling Green, OH 43403, USA, [¶]Dipartimento di Biotecnologie, Chimica e Farmacia, Università di Siena, via A. Moro 2, I-53100 Siena, Italy, [‡]Institut de Physique et Chimie des Matériaux de Strasbourg, UMR 7504 Université de Strasbourg-CNRS, F-67034 Strasbourg, France.

Contents:

- S1: Methodology
- S2: Absorption energies and oscillator strengths
- S3: Comparison of rPSB geometries and cavity residues of ASR_{AT} models
- S4: Evolution of a molecule through a bumpy PES formed by avoided crossings
- S5: Energy profiles computed at the 4-root-state-average level
- S6: Energy and charge profiles of bR models

S1: Methodology

The construction of QM/MM models of ASR and bR was performed following the same protocol that we have employed previously in refs. 1 and 2. In our QM/MM models, the QM and MM subsystems are separated by a hydrogen link atom. The link atom saturates the bond between the last QM atom and the first MM atom of the Lys 210 residue (see Figure S1). The MM subsystem is further divided into fixed and flexible regions where the latter contains protein residues located within 4 Å distance of any QM atom and the former contains the rest of the protein environment. This flexible MM region was allowed to move in all QM/MM calculations. The AMBER force field³ was used to describe both MM regions. With such QM/MM setup the chromophore was optimized on its ground state at state specific CASSCF/6-31G* level with (12, 12) active space. The models hosting artificial rPSB analogues were prepared by simply modifying the native rPSB and carrying out the ground state optimization with the same QM/MM setup as the wild-type. Note that such modifications cause only a minimal perturbation to the cavity (see Figure S2B and C). The oscillator strengths were computed at the 3-root-state-average CASSCF level for the optimized structures. The computed oscillator strengths were used to determine the spectroscopic state and each trajectory was launched on S₁ or S₂. These were 150 fs long and integrated with 1 fs time step. All QM/MM calculations were performed using MOLCAS/TINKER computer package.^{4,5} Consistently with our previous work, the hop of a molecule between two potential energy surfaces was performed using Tully deterministic hop method (~~see section S5~~) in MOLCAS 8.1.⁴ Notice that this is a modified version of widely used Tully surface hop method implemented in MOLCAS (see ref. 4 for more information) where the random number is fixed at a certain value (0.25). The energy profiles along each trajectory were recomputed at CASPT2 level.⁶

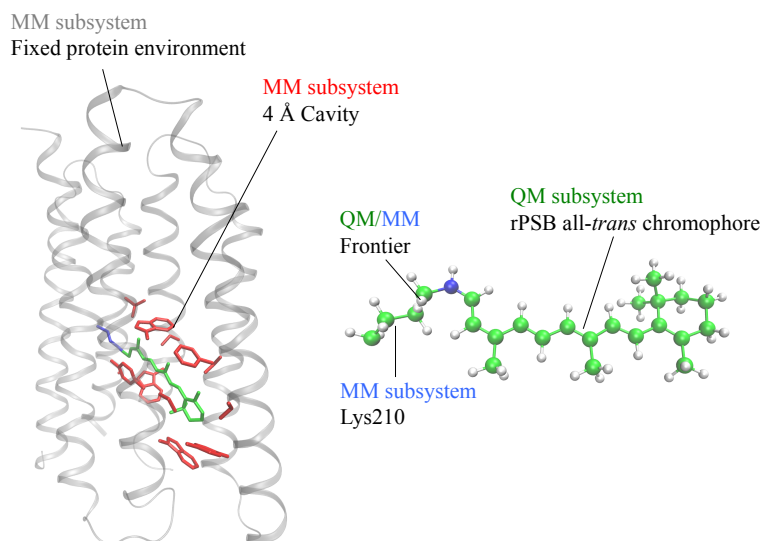


Figure S1. An example of the QM/MM setup (ASR_{13C}) used in the current study. The 13-*cis* chromophore (green) is treated at the QM level. It is bound to MM-subsystem (blue) via a link atom. The amino-acid residues/water molecules located within 4 Å distance of any QM atom (red) are flexible at the MM level. The rest of the environment (grey) is kept frozen at the MM level.

S2: Absorption energies and oscillator strengths

Table S1. Absorption energy (ΔE) and the oscillator strengths (f) computed using each QM/MM mode

	ASR _{AT}	Me-ASR _{AT}	CF3-ASR _{AT}	ASR _{13C}	CF3-ASR _{13C}	bR	CF3-bR
$\Delta E(S_0-S_1)^a$	53.69	65.11	59.52	54.71	61.70	52.99	60.04
$\Delta E(S_0-S_2)^a$	76.93	95.45	74.50	79.51	79.34	77.07	83.58
$f(S_0-S_1)$	1.05	1.1	0.52	0.93	0.67	1.27	0.99
$f(S_0-S_2)$	0.57	0.34	1.12	0.42	0.85	0.39	0.55

^aAbsorption energy is in kcal/mol.

S3: Comparison of rPSB geometries and cavity residues of ASR_{AT} models

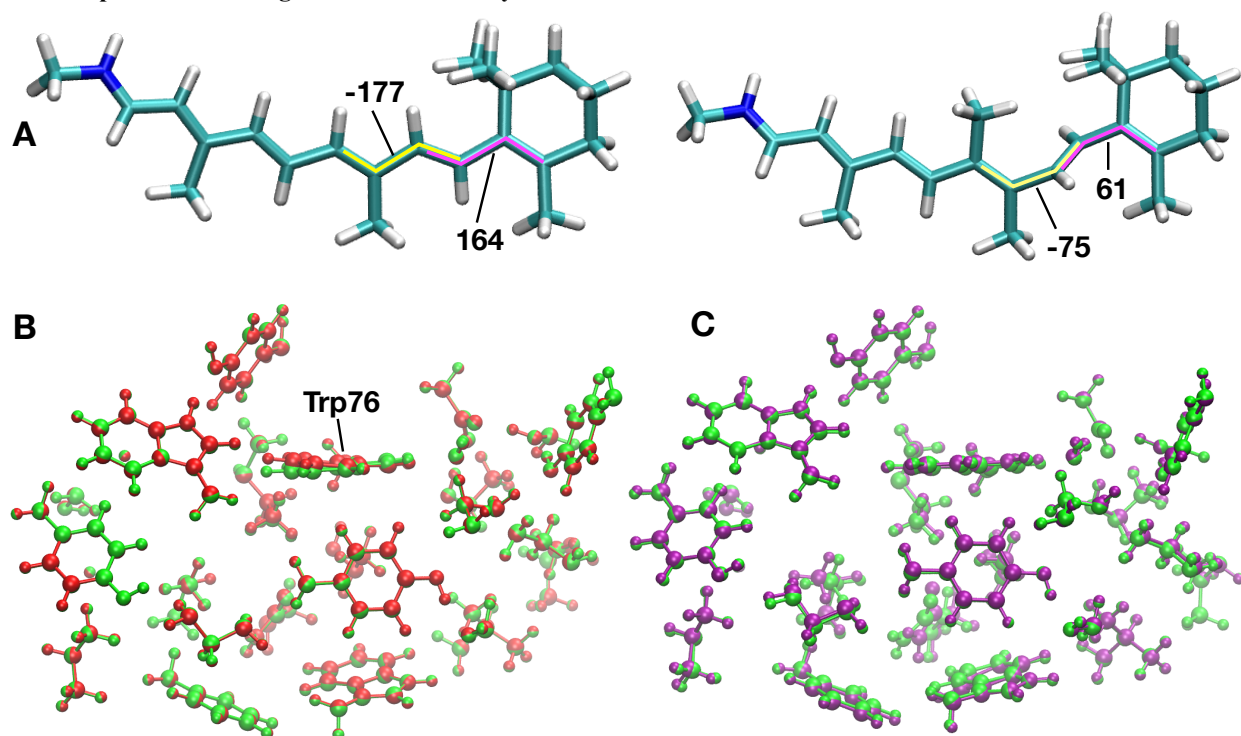


Figure S2. **A.** Comparison of rPSB geometries of ASR_{AT} (left) and Me-ASR_{AT} (right). The reported dihedrals are in degrees. **B.** Comparison of the 4 Å cavities of ASR_{AT} (green) and Me-ASR_{AT} (red) QM/MM models. Note that the retinal chromophore of the has been removed to show the cavity residues clearly. **C.** The same for CF3-ASR_{AT} (purple).

S4: Evolution of a molecule through a bumpy PES formed by avoided crossings

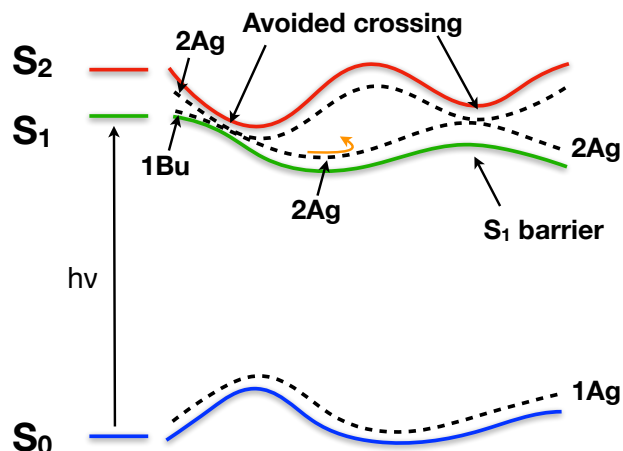


Figure S3. Schematic diagram of PESs driving the photochemical reaction of a system dominated by electronic state mixing. The molecule absorbs light and reaches the S_1 PES having the reactive 1Bu character. As it progresses on S_1 , this PES interacts with S_2 PES resulting in a change of the character of the S_1 wavefunction and is now dominated by unreactive 2Ag character. This results in S_1 barriers and the molecule attempts to overcome such a barrier (denoted by orange arrow) thus leading to a slower photoreactivity.

S5: Energy profiles computed at the 4-root-state-average level

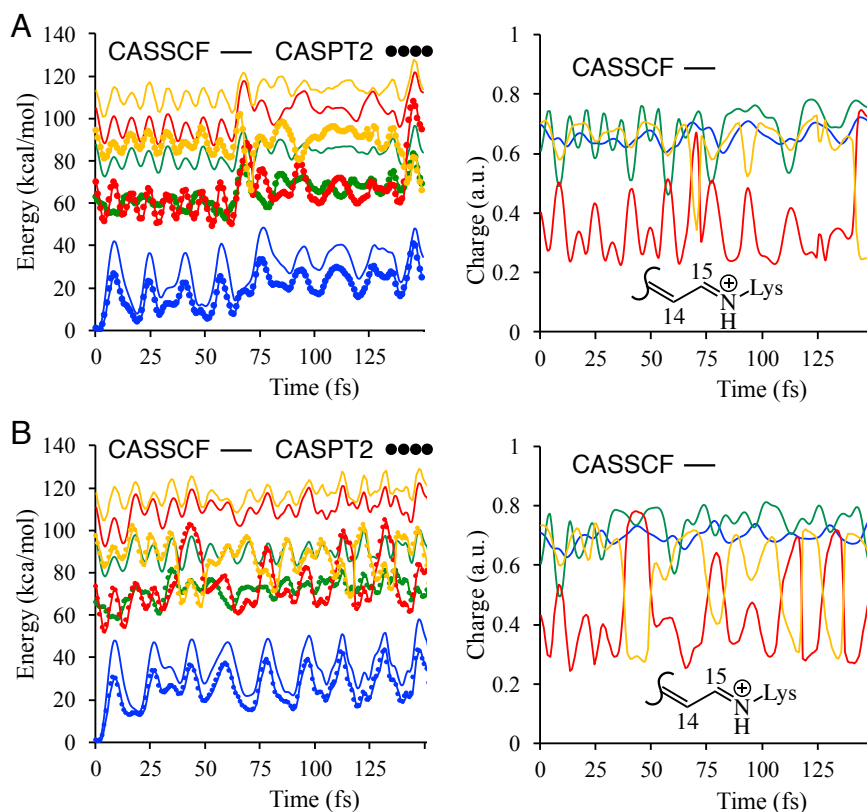


Figure S4. A. 4-root-state-average CASPT2 and CASSCF energies computed along 3-root-state-average CASSCF CF3-ASR_{AT} trajectory (left) and the evolution of Mulliken charge on the displayed rPSB fragment (right). B. Same data for CF3-ASR_{13C}.

S6: Energy and charge profiles of bR models

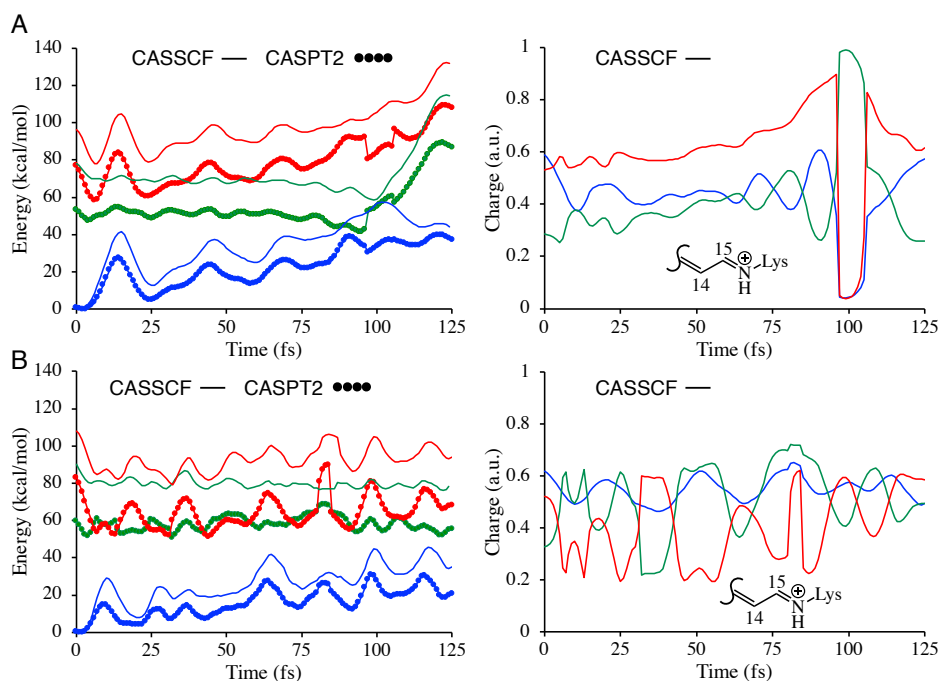



Figure S5. Substituent effect on the relaxation of bR. A. CASSCF and CASPT2 energy profiles (left panel) and evolution of CASSCF charge on the Schiff base side (right panel) of bR. B. Same data for CF3-bR. S_0 , S_1 and S_2 PESs are shown in blue, green and red colors respectively. The profiles shown in the left panels are the positive charge on the displayed molecular fragment 

References

- (1) Manathunga, M.; Yang, X.; Orozco-Gonzalez, Y.; Olivucci, M. Impact of Electronic State Mixing on the Photoisomerization Timescale of the Retinal Chromophore. *J. Phys. Chem. Lett.* **2017**, *8*, 5222–5227.
- (2) Luk, H. L.; Melaccio, F.; Rinaldi, S.; Gozem, S.; Olivucci, M. Molecular Bases for the Selection of the Chromophore of Animal Rhodopsins. *Proc. Natl. Acad. Sci. U. S. A.* **2015**, *112*, 15297–15302.
- (3) Cornell, W. D.; Cieplak, P.; Bayly, C. I.; Gould, I. R.; Merz, K. M.; Ferguson, D. M.; Spellmeyer, D. C.; Fox, T.; Caldwell, J. W.; Kollman, P. A. A Second Generation Force Field for the Simulation of Proteins, Nucleic Acids, and Organic Molecules. *J. Am. Chem. Soc.* **1995**, *117*, 5179–5197.
- (4) Aquilante, F.; Autschbach, J.; Carlson, R. K.; Chibotaru, L. F.; Delcey, M. G.; De Vico, L.; Fdez. Galván, I.; Ferré, N.; Frutos, L. M.; Gagliardi, L.; et al. Molcas 8: New Capabilities for Multiconfigurational Quantum Chemical Calculations across the Periodic Table. *J. Comput. Chem.* **2016**, *37*, 506–541.
- (5) Ponder, J. W.; Richards, F. M. TINKER Molecular Modeling Package. *J. Comput. Chem.* **1987**, *8*, 1016–1024.
- (6) Andersson, K.; Malmqvist, P.-Å.; Roos, B. O. Second-Order Perturbation Theory with a Complete Active Space Self-Consistent Field Reference Function. *J. Chem. Phys.* **1992**, *96*, 1218–1226.